The generalized theory of relativity ...

... gives a correct explanation of the residual motion of the perihelion of planet mercury. As F. Calvo, P. Schwerdtfeger, et al. show in their Communication on page 7583 ff., the special theory of relativity has furnished an even more remarkable result. It gives the correct explanation as to why mercury is the only liquid metal at room temperature, as demonstrated by parallel-tempering Monte Carlo simulations (Picture: Cameron Smorenburg).

Self-Assembly on Surfaces

Borazine-based supramolecular architectures are prepared on a metal surface. A. de Vita, G. Costantini, D. Bonifazi, and co-workers show in their Communication on page 7410 ff. that the structures result from the interplay of van der Waals attractions and Coulomb repulsions.

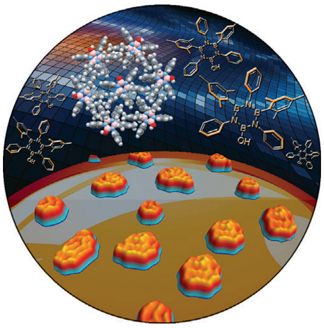

Continuous-Flow Microreactors

In their Communication on page 7564 ff., D.-P. Kim et al. report the development of an automated continuous microfluidic system that produces products through the serial synthesis, purification, and in situ consumption of isocyanides.

Catalytic Olefin Hydrogenation

The metal-free hydrogenation of olefins with $HB(C_6F_5)_2$ as the catalyst is described by Z. H. Li, H. Wang, and co-workers in their Communication on page 7496 ff. The key step in the reaction is a borane-mediated σ-bond metathesis through a four-membered ring transition state.

How to contact us:

Editorial Office:
E-mail: angewandte@wiley-vch.de
Fax: (+49) 6201–606-331
Telephone: (+49) 6201–606-315

Reprints, E-Prints, Posters, Calendars:
Carmen Leitner
E-mail: chem-reprints@wiley-vch.de
Fax: (+49) 6201–606-331
Telephone: (+49) 6201–606-327

Copyright Permission:
Bettina Loycke
E-mail: rights-and-licences@wiley-vch.de
Fax: (+49) 6201–606-332
Telephone: (+49) 6201–606-280

Online Open:
Margitta Schmitt, Carmen Leitner
E-mail: angewandte@wiley-vch.de
Fax: (+49) 6201–606-331
Telephone: (+49) 6201–606-315

Subscriptions:
www.wileycustomerhelp.com
Fax: (+49) 6201–606-184
Telephone: 0800 1800536 (Germany only)
+44(0) 1865476721 (all other countries)

Advertising:
Marion Schulz
E-mail: mschulz@wiley-vch.de
jspiess@wiley-vch.de
Fax: (+49) 6201–606-550
Telephone: (+49) 6201–606-565

Courier Services:
Boschstrasse 12, 69469 Weinheim

Regular Mail:
Postfach 101161, 69451 Weinheim

Angewandte Chemie International Edition is a journal of the Gesellschaft Deutscher Chemiker (GDCh), the largest chemistry-related scientific society in continental Europe. Information on the various activities and services of the GDCh, for example, cheaper subscription to *Angewandte Chemie International Edition*, as well as applications for membership can be found at **www.gdch.de** or can be requested from GDCh, Postfach 900440, D-60444 Frankfurt am Main, Germany.

GDCh
GESELLSCHAFT
DEUTSCHER CHEMIKER

Service

Author Profile

"My biggest motivation is curiosity. Guaranteed to make me smile is when my predictions come true. …"
This and more about Chien-Hong Cheng can be found on page 7348.

News


Z.-J. Shi


G. J. L. Bernardes


C. de Graaf


F. J. Dekker


H. J. Wörner


H. Stegemeyer


E. Neher


B. Sakmann


F. H. Arnold

Meeting Reviews

Books

Highlights

Bioenergetics

Inner workings: The X-ray crystal structure of the entire bacterial complex I at 3.3 Å resolution offers fascinating insights into a giant 536 kDa molecular machine. The respiratory chain complex seems to employ unique mechanisms of energetic coupling that are entirely different from those found in all other enzymes using redox energy to drive vectorial proton transport across a bioenergetic membrane.

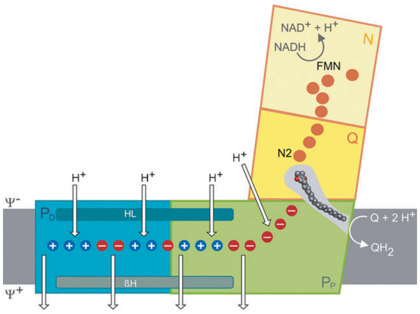

Minireviews

Cross-Coupling

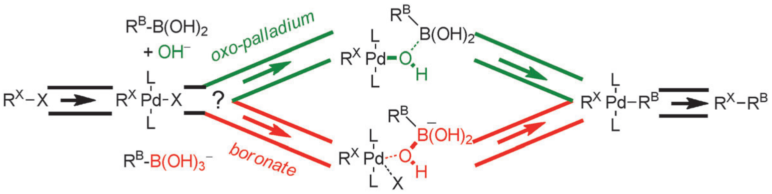

Indecision: The Suzuki–Miyaura coupling is ubiquitous, yet there remains a dichotomy of opinion as to which of two pathways is followed for the delivery of the organoboron component to palladium in the steps leading up to the transmetalation. The importance of deciding between the two pathways should not be underestimated, as it influences the design of optimal conditions for coupling.

For the USA and Canada:
ANGEWANDTE CHEMIE International Edition (ISSN 1433-7851) is published weekly by Wiley-VCH, PO Box 191161, 69451 Weinheim, Germany. Air freight and mailing in the USA by Publications Expediting Inc., 200 Meacham Ave., Elmont, NY 11003. Periodicals postage paid at Jamaica, NY 11431. US POSTMASTER: send address changes to *Angewandte Chemie*, Journal Customer Services, John Wiley & Sons Inc., 350 Main St., Malden, MA 02148-5020. Annual subscription price for institutions: US$ 11.738/10.206 (valid for print and electronic / print or electronic delivery); for individuals who are personal members of a national chemical society prices are available on request. Postage and handling charges included. All prices are subject to local VAT/sales tax.

Reviews

It cuts both ways: The photocatalytic conversion of CO_2 into valuable solar fuels such as methane or methanol has the potential to address the future energy supply demand and mitigate CO_2 emissions. This Review presents the current state of the art of the heterogeneous photocatalytic reduction of CO_2 on TiO_2 and other metal oxides, oxynitrides, sulfides, and phosphides. The mechanisms and the measures of the efficiency of the process are discussed in detail.

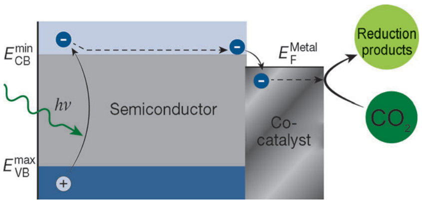

CO_2 Photoreduction

S. N. Habisreutinger, L. Schmidt-Mende,* J. K. Stolarczyk* ______ **7372 – 7408**

Photocatalytic Reduction of CO_2 on TiO_2 and Other Semiconductors

Communications

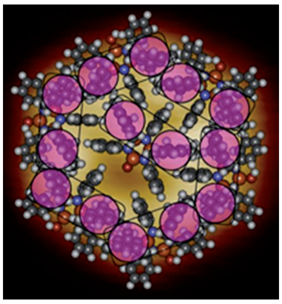

It's a kind of magic: Hydroxy pentaaryl borazine molecules self-assemble into small clusters (see structure) on Cu(111) surfaces, whereas with symmetric hexaaryl borazine molecules large islands are obtained. Simulations indicate that the observed "magic" cluster sizes result from long-range repulsive Coulomb forces arising from the deprotonation of the B–OH groups of the hydroxy pentaaryl borazine.

Self-Assembly on Surfaces

S. Kervyn, N. Kalashnyk, M. Riello, B. Moreton, J. Tasseroul, J. Wouters, T. S. Jones, A. De Vita,* G. Costantini,* D. Bonifazi* ______ **7410 – 7414**

"Magic" Surface Clustering of Borazines Driven by Repulsive Intermolecular Forces

Frontispiece

More than they appear on the surface: The treatment of SiO_2 nanoparticles under mild conditions with two organoboron derivatives led to boron-containing monolayers with different types of surface species (see picture) through the direct formation of Si–O–B bonds. The organoboron-modified SiO_2 NPs showed selective reactivity towards diols.

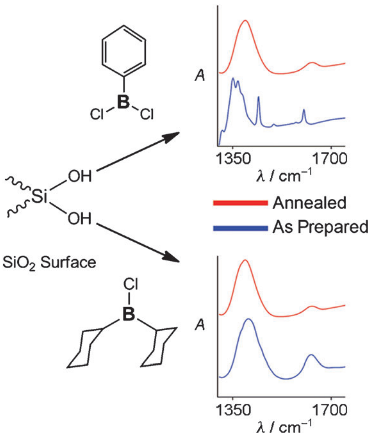

Organoboron Surface Chemistry

A. Agarwala, T. Subramani, A. Goldbourt, D. Danovich, R. Yerushalmi* ______ **7415 – 7418**

Facile Monolayer Formation on SiO_2 Surfaces via Organoboron Functionalities

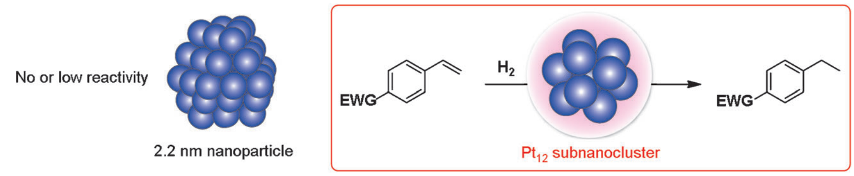

A platinum subnanocluster catalyst composed of 12 atoms was synthesized using a phenylazomethine dendrimer, which can assemble twelve $PtCl_4$ units by stepwise complexation, followed by reduction to Pt^0. Unreactive olefins that were not activated by conventional 2 nm Pt nanoparticles were successfully hydrogenated by the subnanocluster. EWG = electron-withdrawing group.

Nanoclusters

M. Takahashi, T. Imaoka, Y. Hongo, K. Yamamoto* ______ **7419 – 7421**

Formation of a Pt_{12} Cluster by Single-Atom Control That Leads to Enhanced Reactivity: Hydrogenation of Unreactive Olefins

---

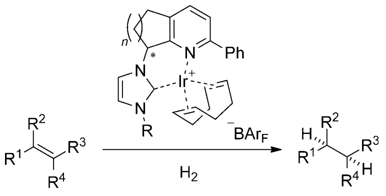

Swapping N,P for C,N: Iridium complexes of bidentate pyridine-based C,N ligands with an N-heterocylic carbene (NHC) unit proved to be efficient and highly enantioselective hydrogenation catalysts. As a result of the lower acidity of iridium hydride intermediates produced from NHC-based complexes, these catalysts are much better suited than analogous N,P-ligand complexes for the hydrogenation of acid-sensitive substrates.

Asymmetric Catalysis

A. Schumacher, M. Bernasconi, A. Pfaltz* ______ **7422 – 7425**

Chiral N-Heterocyclic Carbene/Pyridine Ligands for the Iridium-Catalyzed Asymmetric Hydrogenation of Olefins

---

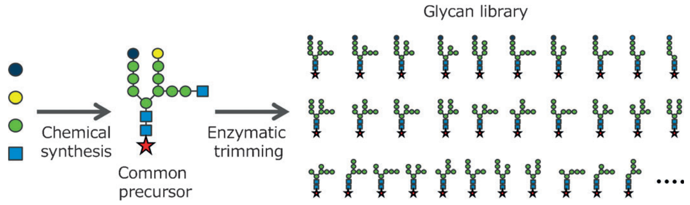

From the stacks: A novel method for construction of a high-mannose-type glycan library by systematic enzymatic trimming of a single synthetic Man_9-based precursor was developed. Efficient chemical synthesis of the tetradecasaccharide common precursor and orthogonal enzymatic trimming to obtain all $M_{8\text{-}9}$ and $G_1M_{8\text{-}9}$ derivatives was demonstrated. G = glucose, M = mannose.

Carbohydrates

A. Koizumi, I. Matsuo, M. Takatani, A. Seko, M. Hachisu, Y. Takeda,* Y. Ito* ______ **7426 – 7431**

Top-Down Chemoenzymatic Approach to a High-Mannose-Type Glycan Library: Synthesis of a Common Precursor and Its Enzymatic Trimming

---

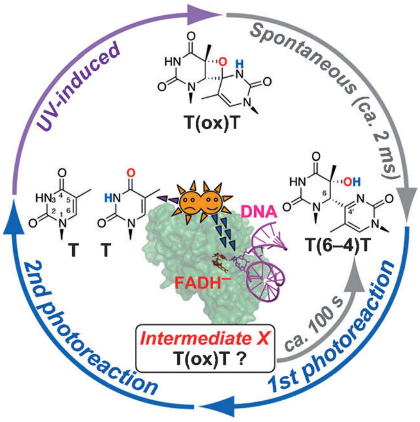

It takes two (photons) to tango: Single-turnover flash experiments showed that the flavoenzyme (6–4) photolyase uses a successive two-photon mechanism to repair the UV-induced T(6–4)T lesion in DNA (see picture). The intermediate (X) formed by the first photoreaction is likely to be the oxetane-bridged dimer T(ox)T. The enzyme could stabilize the normally short-lived T(ox)T, allowing repair to be completed by the second photoreaction.

DNA Repair

J. Yamamoto,* R. Martin, S. Iwai, P. Plaza,* K. Brettel* ______ **7432 – 7436**

Repair of the (6–4) Photoproduct by DNA Photolyase Requires Two Photons

Supramolecular Self-Sorting

C. Talotta, C. Gaeta,* Z. Qi,
C. A. Schalley,* P. Neri* —— **7437 – 7441**

Pseudorotaxanes with Self-Sorted Sequence and Stereochemical Orientation

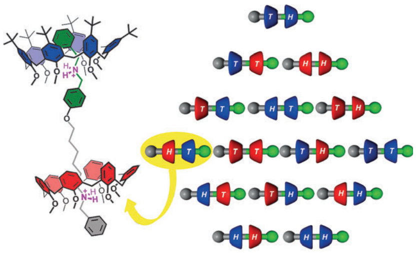

Partner preferences in pseudorotaxane formation were exploited to establish an integrative self-sorting system able to discriminate simultaneously at the sequence and stereochemical level (see picture). It was found that calix[6]arenes were threaded selectively with a preferred orientation onto bisammonium axles, even when the structural differences between the possible building blocks were small and located remote from the binding sites.

Surface Chemistry

W. Xu,* H. Kong, C. Zhang, Q. Sun,
H. Gersen, L. Dong, Q. Tan, E. Lægsgaard,
F. Besenbacher* —————— **7442 – 7445**

Identification of Molecular-Adsorption Geometries and Intermolecular Hydrogen-Bonding Configurations by In Situ STM Manipulation

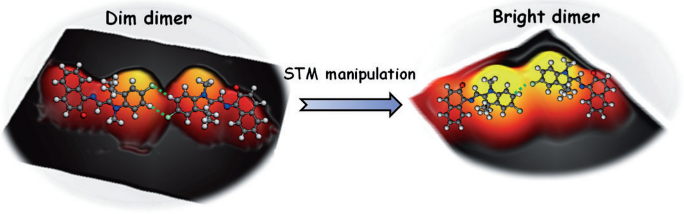

Don't be dim! By combining the technique with DFT calculations, STM manipulation was extended to the probing of intermolecular hydrogen-bonding configurations in self-assembled nanostructures. It was also possible to convert one configuration into another in a controlled fashion through the careful manipulation of a particular structural unit (see picture).

Plasmonic Catalysis

K. Fuku, R. Hayashi, S. Takakura,
T. Kamegawa, K. Mori,
H. Yamashita* —————— **7446 – 7450**

The Synthesis of Size- and Color-Controlled Silver Nanoparticles by Using Microwave Heating and their Enhanced Catalytic Activity by Localized Surface Plasmon Resonance

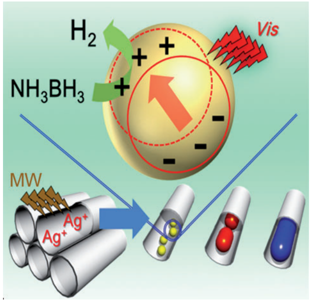

Silver nanoparticles (Ag NPs) of various colors were synthesized within the mesopore structure of SBA-15 by using microwave-assisted alcohol reduction. The charge density is partially localized on the surface of these Ag NPs owing to localized surface plasmon resonance. This charge localization results in them having enhanced catalytic activity under visible light irradiation compared to Ag NPs obtained by thermal processes.

Molecular Imprinting

L. Li, Y. Lu, Z. Bie, H.-Y. Chen,
Z. Liu* ———————— **7451 – 7454**

Photolithographic Boronate Affinity Molecular Imprinting: A General and Facile Approach for Glycoprotein Imprinting

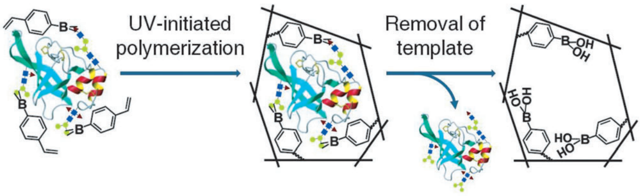

Better than expected: With a regular boronic acid as the functional monomer, a general and facile approach for glycoprotein imprinting exhibited several highly favorable features that are beyond normal expectation, which make the prepared MIPs feasible for the recognition of trace glycoproteins in complicated real samples.

Emulsion Catalysis

H. Q. Yang,* T. Zhou,
W. J. Zhang ______ **7455 – 7459**

A Strategy for Separating and Recycling Solid Catalysts Based on the pH-Triggered Pickering-Emulsion Inversion

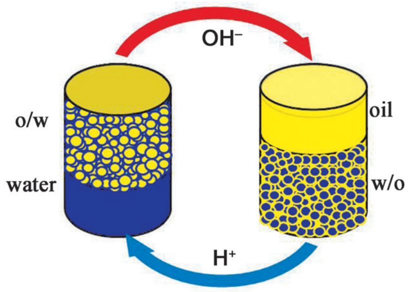

Turn you inside out: A novel method for performing in situ separation and recycling of submicrometer-sized solid catalysts is developed based on the pH-triggered inversion of Pickering emulsions (see scheme; o = oil, w = water). Solid catalysts can be recycled 36 times without significant loss of activity. The method differs from conventional methods in terms of speed, energy consumption, catalyst separation, and recycling effectiveness.

Lithium Batteries

Z. Lin, Z. Liu, W. Fu, N. J. Dudney,
C. Liang* ______ **7460 – 7463**

Lithium Polysulfidophosphates: A Family of Lithium-Conducting Sulfur-Rich Compounds for Lithium–Sulfur Batteries

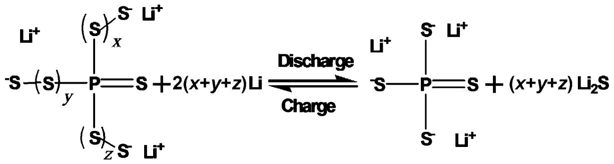

Sulfur-rich lithium polysulfidophosphates (LPSPs) act as an enabler for long-lasting and efficient lithium–sulfur batteries. LPSPs have ionic conductivities of 3.0×10^{-5} S cm^{-1} at 25 °C, which is 8 orders of magnitude higher than that of Li_2S. The high lithium ion conductivity imparts excellent cycling performance, and the batteries are configured in an all-solid state, which promises safe cycling with metallic lithium anodes.

Reaction Dynamics

R. L. Johnson, C. A. Ohlin,* K. Pellegrini,
P. C. Burns, W. H. Casey* ___ **7464 – 7467**

Dynamics of a Nanometer-Sized Uranyl Cluster in Solution

A class of uranyl peroxide clusters was discovered before as nanometer-sized ions that form spontaneously in aqueous solutions. The uranyl(VI) cluster investigated here is approximately 2 nm in diameter, contains 24 uranyl moieties, and 12 pyrophosphate units. NMR spectroscopy shows that the ion has two distinct forms that interconvert in milliseconds to seconds depending on the temperature and the size of the counterions. P blue, O red, U yellow.

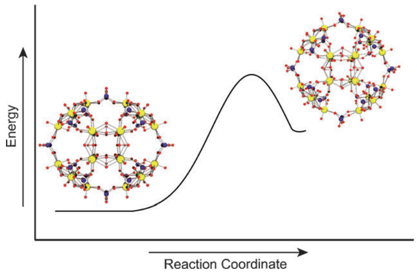

Functional Surfaces

T. Masuda, M. Hidaka, Y. Murase,
A. M. Akimoto, K. Nagase, T. Okano,
R. Yoshida* ______ **7468 – 7471**

Self-Oscillating Polymer Brushes

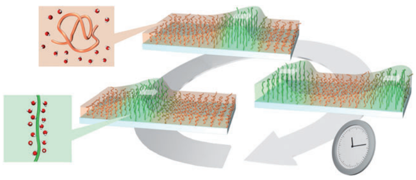

An autonomous functional surface has been designed by using self-oscillating polymers that convert the chemical energy of the Belousov–Zhabotinsky reaction into conformational changes of the polymer chains (see picture: red: hydrophobic/collapsed, green: hydrophilic/extended). Self-oscillating polymer brushes were grafted onto the inner surface of a glass capillary, and autonomous propagation of a chemical wave was observed.

Electrocatalysts

H. H. Li, S. Zhao, M. Gong, C. H. Cui,
D. He, H. W. Liang, L. Wu,
S. H. Yu* ______________ **7472 – 7476**

Ultrathin PtPdTe Nanowires as Superior Catalysts for Methanol Electrooxidation

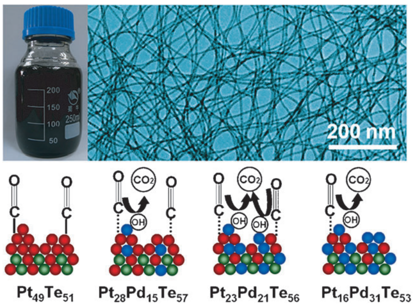

Ultrathin and ultralong: Highly uniform, ultrathin (diameter 5–7 nm), and ultralong (aspect ratio $> 10^4$) PtPdTe nanowires (NWs) were synthesized by using a facile method employing Te NWs as both sacrificial templates and reducing agents. Fine-tuning of the molar ratios of Pt and Pd precursors afforded PtPdTe NWs with different compositions and enhanced electroactivity in the methanol oxidation reaction in comparison with a commercial Pt/C catalyst.

Proteomics

A. Beloqui, J. Calvo, S. Serna, S. Yan,
I. B. H. Wilson, M. Martin-Lomas,
N. C. Reichardt* ___________ **7477 – 7481**

Analysis of Microarrays by MALDI-TOF MS

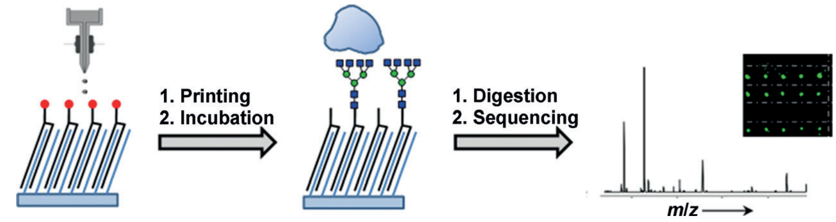

Ligand libraries can be printed onto a sandwich composed of activated lipids embedded in a hydrophobic layer conjugated to an indium–tin oxide (ITO) surface. Arrays produced this way can be analyzed by fluorescence spectroscopy and mass spectrometry. Applications include the assignment of enzyme specificity, the profiling of glycoforms and the identification of lectins.

Supramolecular Chemistry

C. Shao, M. Stolte,
F. Würthner* ______________ **7482 – 7486**

Quadruple π Stack of Two Perylene Bisimide Tweezers: A Bimolecular Complex with Kinetic Stability

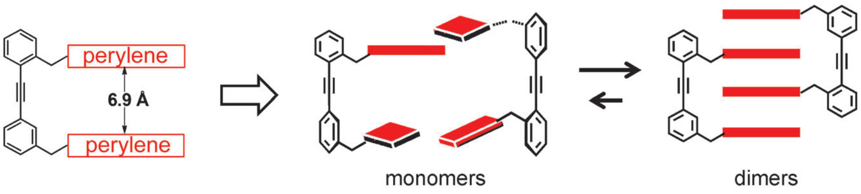

Self-assembly: A tweezer-type perylene bisimide (PBI) dyad self-assembles into a defined bimolecular complex composed of a quadruple PBI π stack with remarkable kinetic stability, which is unprecedented for π-stacked dye aggregates (see picture). These persistent supramolecular species are of considerable interest for the elucidation of functional properties of dye aggregates.

Drug Delivery

Z. Zhao, H. Meng, N. Wang,
M. J. Donovan, T. Fu, M. You, Z. Chen,
X. Zhang,* W. Tan* _________ **7487 – 7491**

A Controlled-Release Nanocarrier with Extracellular pH Value Driven Tumor Targeting and Translocation for Drug Delivery

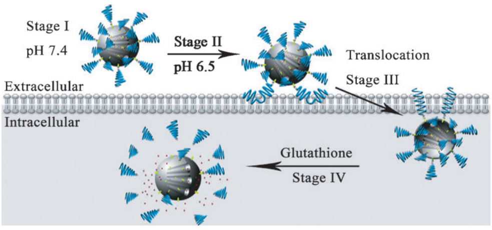

This pHLIP is no flop: Functionalizing mesoporous silica nanoparticles (MSNs) with pHLIPss peptide provides a controlled-release nanoparticle drug delivery system targeting the acidic tumor microenvironment. At low pH values, pHLIPss inserts into the cell membrane and translocates carriers into cells, where the cargo is released by the cleavage of the pHLIPss disulfide bonds (see scheme).

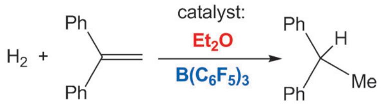

It works ether way: Labile adducts of dialkyl ethers with the electrophilic borane $B(C_6F_5)_3$ are shown to scramble HD to H_2 and D_2 and catalyze the hydrogenation of 1,1-diphenylethylene.

Frustrated Lewis Pairs

L. J. Hounjet, C. Bannwarth, C. N. Garon, C. B. Caputo, S. Grimme,* D. W. Stephan* ________ **7492 – 7495**

Combinations of Ethers and $B(C_6F_5)_3$ Function as Hydrogenation Catalysts

---

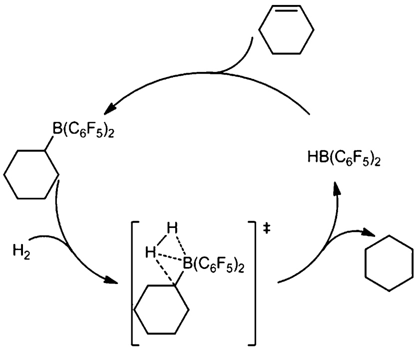

Out with the metal: Metal-free hydrogenation of unfunctionalized olefins can be achieved by employing $HB(C_6F_5)_2$ as the catalyst. The key step in the catalytic reaction is believed to involve a novel borane-mediated σ-bond metathesis, which has been investigated both experimentally and theoretically.

Synthetic Methods

Y. Wang, W. Chen, Z. Lu, Z. H. Li,* H. Wang* ________ **7496 – 7499**

Metal-Free $HB(C_6F_5)_2$-Catalyzed Hydrogenation of Unfunctionalized Olefins and Mechanism Study of Borane-Mediated σ-Bond Metathesis

Back Cover

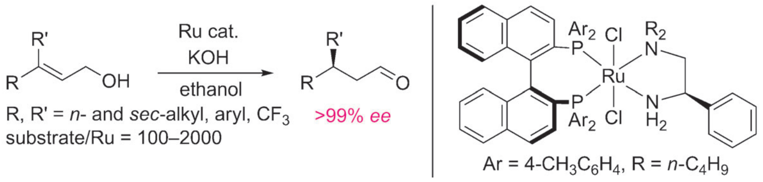

Efficient isomerization: The title reaction was catalyzed by the $[RuCl_2\{(S)\text{-tol-binap}\}\{(R)\text{-dbapen}\}]$/KOH system in ethanol at 25 °C (see scheme). A series of *E*- and *Z*-configured aromatic and aliphatic allylic alcohols, including a simple primary alkyl-substituted compound (*E*)-3-methyl-2-hepten-1-ol, were transformed into the chiral aldehydes with at least 99 % *ee*. dbapen = 2-dibutylamino-1-phenylethylamine, tol-binap = 2,2′-bis(di-4-tolylphosphanyl)-1,1′-binaphthyl.

Asymmetric Catalysis

N. Arai, K. Sato, K. Azuma, T. Ohkuma* ________ **7500 – 7504**

Enantioselective Isomerization of Primary Allylic Alcohols into Chiral Aldehydes with the tol-binap/dbapen/Ruthenium(II) Catalyst

Inside Cover

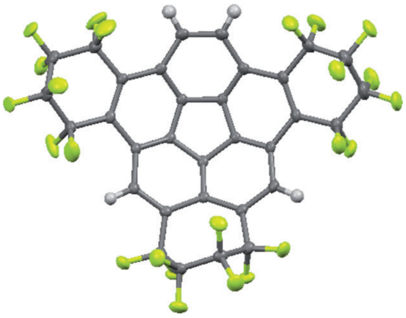

At sixes and sevens: The reaction of corannulene with 35 equivalents of 1,4-$C_4F_8I_2$ is an efficient and a relatively selective process that yields two main products in which six H atoms are substituted with three C_4F_8 moieties that form six- and seven-membered rings. Low-temperature photoelectron spectroscopy showed the electron affinity of the major isomer (shown) exceeds that of C_{60} (2.74 ± 0.02 and 2.689 ± 0.008 eV, respectively).

Electron Acceptors

I. V. Kuvychko,* C. Dubceac, S. H. M. Deng, X. B. Wang,* A. A. Granovsky, A. A. Popov,* M. A. Petrukhina,* S. H. Strauss,* O. V. Boltalina* ________ **7505 – 7508**

$C_{20}H_4(C_4F_8)_3$: A Fluorine-Containing Annulated Corannulene that Is a Better Electron Acceptor Than C_{60}

Synthetic Methods

I. Thomé, C. Besson, T. Kleine,
C. Bolm* ———— 7509 – 7513

Base-Catalyzed Synthesis of Substituted Indazoles under Mild, Transition-Metal-Free Conditions

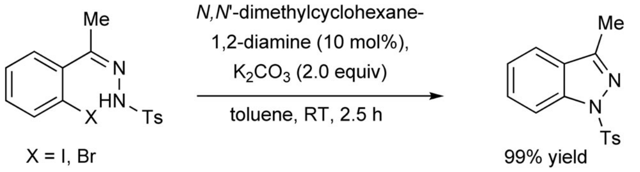

Back to basics: A transition-metal-free method developed for the synthesis of indazoles involves an inexpensive catalytic system composed of a diamine and K_2CO_3. Various (*Z*)-2-bromoacetophenone tosylhydrazones were converted into indazoles at room temperature in excellent yields (see example; Ts = *p*-toluenesulfonyl). The yield was improved by photoisomerization with UV light when *E*/*Z* isomeric mixtures of the starting material were used.

Photocatalysts

J. E. Yoo, K. Lee, M. Altomare, E. Selli,
P. Schmuki* ———— 7514 – 7517

Self-Organized Arrays of Single-Metal Catalyst Particles in TiO_2 Cavities: A Highly Efficient Photocatalytic System

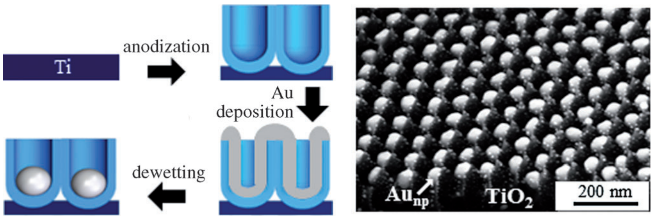

Peas in a pod: A highly aligned $Au_{np}@TiO_2$ photocatalyst was formed by self-organizing anodization of a Ti substrate followed by dewetting of a gold thin film. This leads to exactly one Au nanoparticle (np) per TiO_2 nanocavity. Such arrays are highly efficient photocatalysts for hydrogen generation from ethanol.

Alkene Synthesis

J. R. Lawson, E. R. Clark, I. A. Cade,
S. A. Solomon,
M. J. Ingleson* ———— 7518 – 7522

Haloboration of Internal Alkynes with Boronium and Borenium Cations as a Route to Tetrasubstituted Alkenes

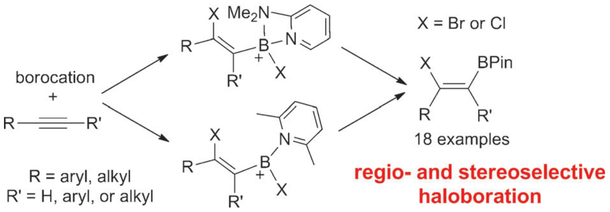

Hail boration! 2-Dimethylaminopyridine-ligated dihaloborocations $[X_2B(2\text{-DMAP})]^+$ with a strained four-membered boracycle were used for the haloboration of terminal and dialkyl internal alkynes (see scheme). Esterification then provided vinyl boronate esters as useful precursors to tetrasubstituted alkenes. Following mechanistic studies, the scope of the haloboration was expanded simply by variation of the amine. Pin = 2,3-dimethyl-2,3-butanedioxy.

Homogeneous Catalysis

S. Chakraborty, Y. J. Patel, J. A. Krause,
H. Guan* ———— 7523 – 7526

A Robust Nickel Catalyst for Cyanomethylation of Aldehydes: Activation of Acetonitrile under Base-Free Conditions

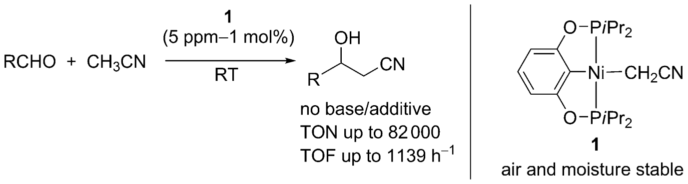

Nick of time: The nickel cyanomethyl complex **1** catalyzes the room temperature coupling of aldehydes with acetonitrile under base-free conditions. The catalytic system is long-lived and remarkably efficient with high turnover numbers (TONs) and turnover frequencies (TOFs) achieved. The mild reaction conditions allow a wide variety of aldehydes, including base-sensitive ones, to catalytically react with acetonitrile.

B,N Heterocycles

S. Xu, T. C. Mikulas, L. N. Zakharov, D. A. Dixon, S.-Y. Liu* ______ **7527 – 7531**

Boron-Substituted 1,3-Dihydro-1,3-azaborines: Synthesis, Structure, and Evaluation of Aromaticity

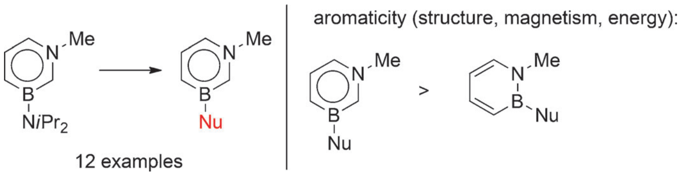

Getting the family together: A general synthetic strategy based on nucleophilic substitution provided B-substituted 1,3-dihydro-1,3-azaborines (see scheme), BN isosteres of arenes with potential for application in biomedicine and materials science. Experimental structural analysis and calculations suggest that the aromaticity of the 1,3-dihydro-1,3-azaborine heterocycle is intermediate between that of benzene and that of 1,2-dihydro-1,2-azaborine.

Asymmetric Catalysis

J. Y. Hamilton, D. Sarlah, E. M. Carreira* ______ **7532 – 7535**

Iridium-Catalyzed Enantioselective Allylic Alkynylation

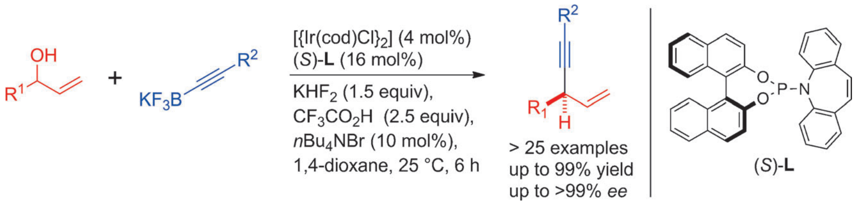

No leaving group needed: With an Ir-(P,olefin) complex as catalyst, the direct enantioselective allylic alkynylation of secondary allylic alcohols with potassium alkynyltrifluoroborates as alkynylating reagents has been achieved. High levels of enantioselectivity and high yields were achieved with this operationally easy and robust protocol, the use of which was demonstrated in the synthesis of GPR40 receptor agonist AMG 837. cod = 1,5-cyclooctadiene.

Heterocycles

I. Nakamura,* Y. Kudo, M. Terada ______ **7536 – 7539**

Oxazepine Synthesis by Copper-Catalyzed Intermolecular Cascade Reactions between O-Propargylic Oximes and Dipolarophiles

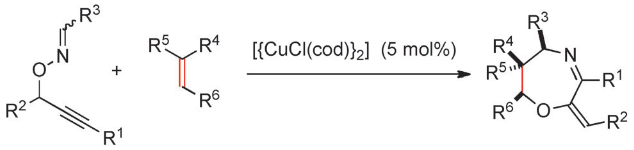

Three-step cascade: Oxazepine derivatives were efficiently prepared from O-propargylic oximes and dipolarophiles through copper-catalyzed cascade reactions which proceed through a 2,3-rearrangement, [3+2] cycloaddition, and subsequent 1,3-oxygen rearrangement. The process involves the cleavage of C–O and N–O bonds.

Asymmetric Catalysis

G. Yang, W. Zhang* ______ **7540 – 7544**

A Palladium-Catalyzed Enantioselective Addition of Arylboronic Acids to Cyclic Ketimines

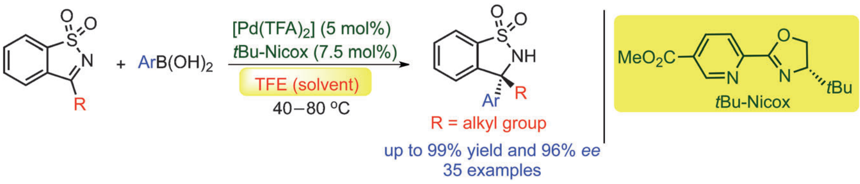

Sly as Nicox: A palladium-catalyzed addition of arylboronic acids to ketimines has been developed to efficiently provide products in up to 99 % yield and 96 % *ee*. The reactions could be run under aerobic conditions and with unpurified trifluoroethanol (TFE). A pyrrolidine compound bearing a chiral α-tertiary amine was synthesized in several steps without loss of enantioselectivity. TFA = trifluoroacetate.

Photovoltaics

Z. Yang, H. Sun, T. Chen, L. Qiu, Y. Luo,
H. Peng* ________ 7545 – 7548

Photovoltaic Wire Derived from a Graphene Composite Fiber Achieving an 8.45 % Energy Conversion Efficiency

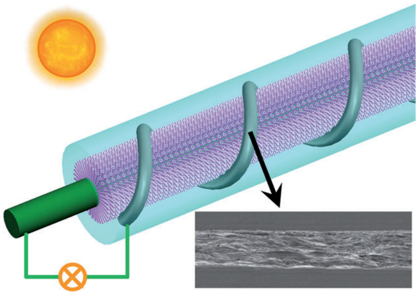

Wired for light: Novel wire-shaped photovoltaic devices have been developed from graphene/Pt composite fibers. The high flexibility, mechanical strength, and electrical conductivity of graphene composite fibers resulted in a maximum energy conversion efficiency of 8.45 %, which is much higher than that of other wire-shaped photovoltaic devices.

Synthetic Methods

Z. Zhang, F. Wang, X. Mu, P. Chen,
G. Liu* ________ 7549 – 7553

Copper-Catalyzed Regioselective Fluorination of Allylic Halides

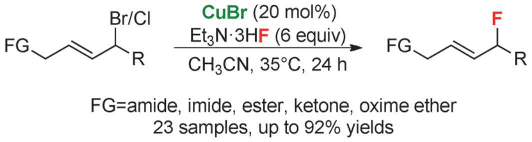

Group activity: A novel copper-catalyzed fluorination of internal allylic bromides and chlorides has been developed by using $Et_3N\cdot3HF$ as the fluorine source. A functional group (FG) within the substrate is required to achieve the allylic fluorination, and a variety of secondary allylic fluoride compounds can be accessed in good yield with excellent regioselectivity.

Nanosheets

T. Yao, L. Liu, C. Xiao, X. D. Zhang,
Q. H. Liu, S. Q. Wei,*
Y. Xie* ________ 7554 – 7558

Ultrathin Nanosheets of Half-Metallic Monoclinic Vanadium Dioxide with a Thermally Induced Phase Transition

Only the half of it: A modified intercalation–deintercalation strategy that takes advantage of the characteristic thermally induced phase transition of monoclinic VO_2 has been developed for the preparation of ultrathin VO_2 nanosheets. The resultant nanosheets exhibit half-metallic character and a temperature-dependent phase transition. The half-metallicity could lead to applications in spintronic nanodevices.

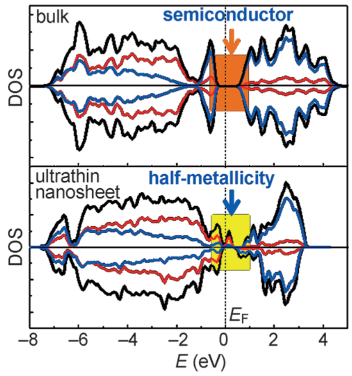

Synthetic Methods

S. K. Pawar, C.-D. Wang, S. Bhunia,
A. M. Jadhav, R.-S. Liu* ____ 7559 – 7563

Gold-Catalyzed Formal Cycloaddition of 2-Ethynylbenzyl Ethers with Organic Oxides and α-Diazoesters

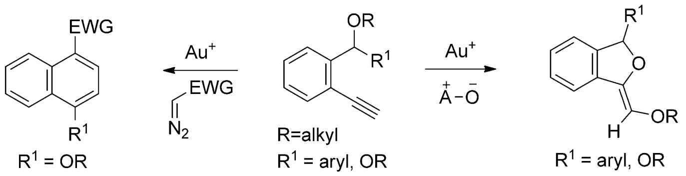

A world of possibilities: Gold-catalyzed reactions of 2-ethynylbenzyl ethers with organic oxides and α-diazoesters gave 1,3-dihydroisobenzofuran and naphthalene derivatives, respectively (see scheme; EWG = electron-withdrawing group). Mechanisms for the formation of the formal cycloadducts were elucidated by isotope labeling.

Continuous-Flow Microreactors

S. Sharma, R. A. Maurya, K.-I. Min, G.-Y. Jeong, D.-P. Kim* ____ **7564 – 7568**

Odorless Isocyanide Chemistry: An Integrated Microfluidic System for a Multistep Reaction Sequence

Inside Back Cover

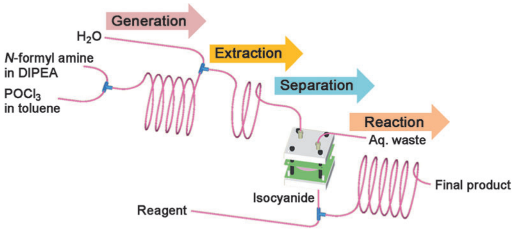

Can't smell this: An integrated continuous-flow microfluidic setup enables in situ generation, extraction, separation, and reaction of foul-smelling isocyanides with little exposure to the surroundings. Isocyanides were generated by dehydration of the corresponding N-substituted formamides, and several representative isocyanide-based organic reactions were successfully performed. DIPEA = *N*,*N*-diisopropylethylamine.

Natural Product Synthesis

Y. Kobayakawa, M. Nakada* **7569 – 7573**

Total Syntheses of (−)-Scabronines G and A, and (−)-Episcabronine A

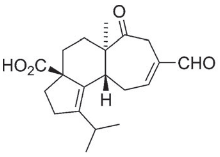

(−)-scabronine G
19 steps, 21%

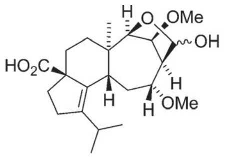

(−)-scabronine A
27 steps, 10%

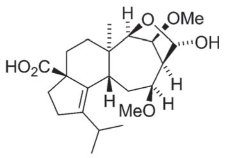

(−)-episcabronine A
27 steps, 13%

Making scab(ronine)s: The total synthesis of (−)-scabronine G features a highly stereoselective oxidative dearomatization/intramolecular inverse-electron-demand Diels–Alder reaction cascade, and the first total synthesis of (−)-scabronine A comprises a highly stereoselective oxa-Michael/protonation/acetalization cascade. The first total synthesis of (−)-episcabronine A includes another highly stereoselective cascade.

Radical Reactions

J. Peng, C. Chen,* Y. Wang, Z. Lou, M. Li, C. Xi, H. Chen* ________ **7574 – 7578**

Direct Vicinal Disubstitution of Diaryliodonium Salts by Pyridine *N*-oxides and *N*-amidates by a 1,3-Radical Rearrangement

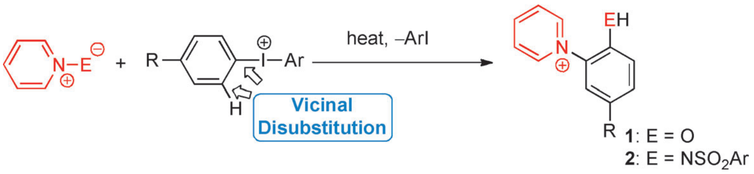

Paired off: The title reaction leads to a series of *o*-pyridinium phenols (**1**) and anilines (**2**). The experimental and computational studies indicate that the key step involves homolytic cleavage to give a radical pair, which undergoes solvent-cage recombination to give the product.

Alkyne Halosilylation

N. T. Barczak, D. A. Rooke, Z. A. Menard, E. M. Ferreira* ________ **7579 – 7582**

Stereoselective Synthesis of Tetrasubstituted Olefins through a Halogen-Induced 1,2-Silyl Migration

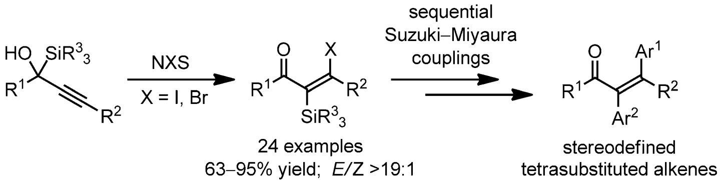

Migrating through Si valley: The highly stereoselective formation of α-silyl-β-haloenones by way of silicon group migration is described. Electrophilic activation of the alkyne by *N*-halosuccinimides induced an *anti*-selective migration to give highly substituted enones (see scheme). These enone products can be readily converted to the all-carbon tetrasubstituted alkenes while maintaining their geometry.

Relativistic Effects

F. Calvo,* E. Pahl, M. Wormit,
P. Schwerdtfeger* ———— 7583 – 7585

Evidence for Low-Temperature Melting of Mercury owing to Relativity

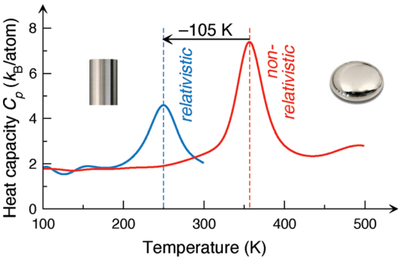

An old problem solved: Monte Carlo simulations using the diatomic-in-molecule method derived from accurate ground- and excited-state relativistic calculations for Hg_2 show that the melting temperature for bulk mercury is lowered by 105 K, which is due to relativistic effects.

Front Cover

Gold Catalysis

Y. Yu, W. Yang, F. Rominger,
A. S. K. Hashmi* ———— 7586 – 7589

In Situ Generation of Nucleophilic Allenes by the Gold-Catalyzed Rearrangement of Propargylic Esters for the Highly Diastereoselective Formation of Intermolecular C(sp^3)—C(sp^2) Bonds

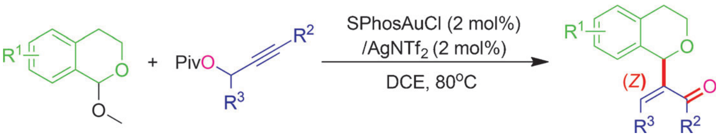

New perspectives, in particular for the synthesis of isochromane derivatives (see scheme), are provided by the title reaction. Excellent diastereoselectivites are achieved in this reaction which proceeds through a gold-catalyzed 1,3-acyloxy migration. In some cases exclusively the *Z* isomer is detected.

Nucleophilic Boron

D. A. Ruiz, G. Ung, M. Melaimi,
G. Bertrand* ———— 7590 – 7592

Deprotonation of a Borohydride: Synthesis of a Carbene-Stabilized Boryl Anion

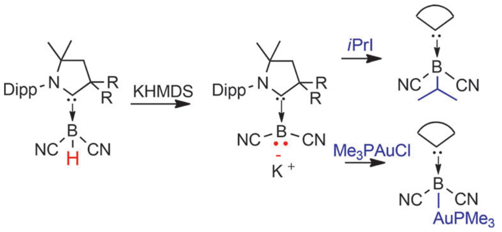

An acidic hydride! Thanks to the presence of a π-acceptor cyclic alkyl amino carbene and of two electron-withdrawing nitrile groups, a borohydride reacts with a base to give a carbene-stabilized boryl anion, which reacts with carbon and metal electrophiles at the boron center. Dipp = 2,6-diisopropylphenyl, KHMDS = potassium bis(trimethylsilyl)amide.

Bioinorganic Chemistry

S. V. Wegner, J. P. Spatz* —— 7593 – 7596

Cobalt(III) as a Stable and Inert Mediator Ion between NTA and His6-Tagged Proteins

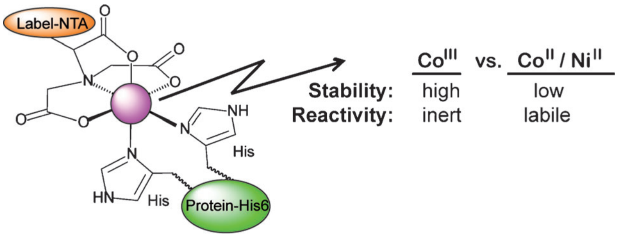

Don't let go! The Co^{3+}-mediated interaction between nitrilotriacetic acid (NTA) and the His6-tag is so stable and inert towards ligand exchange that it has a half-life of 7 days in the presence of imidazole and survives even under strongly chelating as well as reducing conditions, unlike the commonly used Ni^{2+} or Co^{2+} complexes. Possible applications include the separation of labeled proteins and the stable immobilization of proteins on surfaces.

A novel concept to release peptidic drugs systemically by serum proteases from a PEGylated precursor makes it possible to tune release kinetics to fit the medical needs. Drug release depends on the size of the PEG polymer and the sequence and length of the peptide linker. The antimicrobial activities of the prodrugs were even better than those of the free peptides, whereas direct PEGylation abolished the peptide activity.

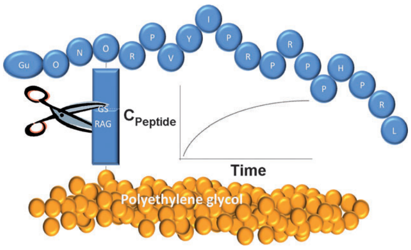

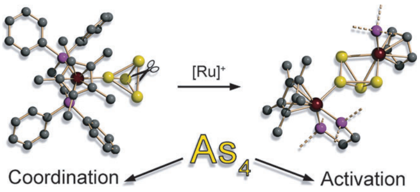

One time only: The reaction of [Cp*Ru(dppe)Cl] with the potent As_4 transfer reagent $[Ag(\eta^2\text{-}As_4)_2]^+[pftb]^-$ leads to $[Cp^*Ru(dppe)(\eta^1\text{-}As_4)]^+[pftb]^-$ with an unprecedented end-on-coordinated As_4 tetrahedron. Reaction with a second cationic ruthenium complex fragment does not lead to a second end-on coordination but to the cleavage of one basal As–As bond. This behavior, which differs from its phosphorus analogues, is rationalized by DFT calculations.

Supporting information is available on www.angewandte.org (see article for access details).

A video clip is available as Supporting Information on www.angewandte.org (see article for access details).

This article is available online free of charge (Open Access).

This article is accompanied by a cover picture (front or back cover, and inside or outside).

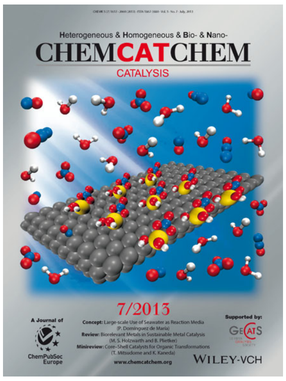

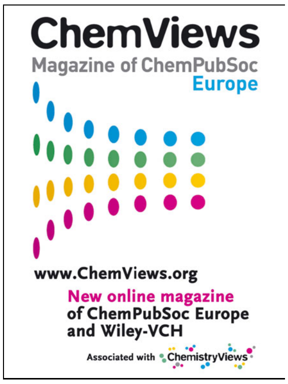

Angewandte Corrigendum

Shape Control of Thermodynamically Stable Cobalt Nanorods through Organometallic Chemistry

F. Dumestre, B. Chaudret,* C. Amiens,
M.-C. Fromen, M.-J. Casanove,
P. Renaud, P. Zurcher ____ **4286–4289**

Angew. Chem. Int. Ed. **2002**, *41*

DOI: 10.1002/1521-3773(20021115)41:22<4286::AID-ANIE4286>3.0.CO;2-M

The magnetization plot shown in Figure 3 a of this Communication was measured at 2 K, and not at 300 K, as erroneously stated in the caption.

Angewandte Corrigendum

Highly Enantioselective Catalytic [6+3] Cycloadditions of Azomethine Ylides

M. Potowski, J. O. Bauer,
C. Strohmann, A. P. Antonchick,*
H. Waldmann* ________ **9512–9516**

Angew. Chem. Int. Ed. **2012**, *51*

DOI: 10.1002/anie.201204394

In this Communication, the headline for column 5 of Table 2 is incorrect. The correct headline is "*endo*/*exo*". This corresponds to an *endo*-selective Diels–Alder reaction. The authors sincerely apologize for this mistake.